



Accepted Author Manuscript

Journal: *Applied Optics*

Article Title: Flatness parameter influence on scintillation reduction for multi-Gaussian Schell-model beams propagating in turbulent air

Authors: S. Avramov-Zamurovic, C. Nelson, S. Guth, and O. Korotkova

Accepted for publication: 16 March 2016

Final version published: 22 April 2016

DOI: <http://dx.doi.org/10.1364/AO.55.003442>

Access to this article is made available via **CHORUS** and subject to [OSA Publishing Terms of Use](#).

Flatness parameter influence on scintillation reduction for Multi-Gaussian Schell-Model beams propagating in turbulent air

S. AVRAMOV-ZAMUROVIC^{1*}, C. NELSON², S. GUTH³, O. KOROTKOVA⁴

¹ Weapons and Systems Engineering Department, US Naval Academy, 105 Maryland Avenue, Annapolis, MD 21402, USA

² Electrical and Computer Engineering Department, US Naval Academy, 105 Maryland Avenue, Annapolis, MD 21402, USA

³ Mathematics Department, US Naval Academy, 589 McNair Rd, Stop 10M, Annapolis MD 21402, USA

⁴ Department of Physics, University of Miami, 1320 Campo Sano Dr., Coral Gables FL 33146, USA

*Corresponding author: avramov@usna.edu

Received XX Month XXXX; revised XX Month, XXXX; accepted XX Month XXXX; posted XX Month XXXX (Doc. ID XXXXX); published XX Month XXXX

Reduction in the scintillation index of Multi-Gaussian Schell-model beams propagating in turbulent air is demonstrated as a function of two source parameters: the r.m.s. coherence width and the summation index. The beams were generated with the help of a nematic phase-only, reflective spatial light modulator at a cycling rate of 333 frames per second and recorded after propagating through a weakly turbulent air channel over a distance of 70 meters. Experimental results are in good agreement with theory.

OCIS codes: 010.1300) Atmospheric propagation; (010.1330) Atmospheric turbulence; (060.2605) Free-space optical communication; (030.7060) Turbulence; (290.5930) Scintillation

<http://dx.doi.org/10.1364/AO.99.099999>

1. INTRODUCTION

For mitigation of turbulent atmosphere, in terms of reduction of intensity fluctuations (scintillations) in optical links, various approaches have been employed: aperture averaging [1], receiver arrays [2], as well as spectral and polarization diversification [3, 4]. The fine control of spatial partial coherence of the source has also been successfully demonstrated both theoretically and experimentally to lead to suppression of scintillations [5-13]. So far, the majority of work has been dedicated to the coherence properties of the classic Gaussian Schell Model (GSM) sources, characterized by one coherence-related parameter, r.m.s. (typical) coherence width. It has been shown that the GSM sources can be optimized with respect to this parameter, which takes a certain value for a given atmospheric channel in order to minimize the scintillation index [9]. For values smaller than the optimal, the beam diverges too fast, and for values larger than the optimal the partial coherence is under-utilized.

Recently, a variety of random sources with non-Gaussian shapes of the degree of coherence have been introduced [14-20]. The beams radiated by such sources can form practically arbitrary average intensity distributions in the far zone on propagation in free space. On passing through the turbulent air the beams with these special source coherence characteristics can form the prescribed average intensity patterns at certain distances from the source plane, which gradually convert to Gaussian-like intensity patterns with further propagation [21-25]. In particular, the Multi-Gaussian Schell-Model (MGSM)

sources have been shown to produce flat circular intensity profiles at the beam center with Gaussian decay at the beam edges [15, 16]. This feature can be employed in any application where power-optimized, uniform illumination of circular distant objects is required. The MGSM beams are mathematically described as a two-parametric model: one parameter is the r.m.s. coherence width (just like for the GSM beams) and the other is the number of terms in summation relating to beam size and flatness. A recent theoretical investigation of the scintillation index for the MGSM beams on propagation in turbulent air has shown that with an increase of the flatness parameter (and with a fixed coherence width parameter) the scintillation index must monotonically decrease [26]. Such a result implies that not only the width of the source coherence function, but also its spatial profile can influence the intensity fluctuations. In this paper we provide the experimental justification for this theoretical prediction (see also [27] where our preliminary results have been reported).

The random beams with spatial correlation functions may be produced with the help of holograms [28-30] or spatial light modulators (SLM) [31-33]. In our experimental setup we employ a commercial phase-only, nematic, reflective SLM with high spatial resolution and high temporal turnover rate. In creating the phase screens we have followed the procedure discussed in details in Refs [31 - 33, 35, 36]. The turbulent air channel that the beam propagated through had a range of 70 meters and a C_r^2 of approximately $10^{-14}\text{m}^{-2/3}$.

Partially coherent beams can only be a solution to the "last mile" problem, i.e. they are only applicable for relatively short links with weak turbulence. For larger distances with stronger turbulence the

divergence of the partially coherent beams becomes too large and power in the bucket too small, regardless of the scintillation level. This paper illustrates the reduction in scintillation index only for short links for which the scintillation is reduced, but the divergence is still small.

The paper is organized as follows; Section 2 addresses generation of MGSM beams and the data analysis. Section 3 lays out the experimental set-up and the procedure and Section 4 gives the results. Section 5 summarizes our findings.

2. MULTI-GAUSSIAN SCHELL-MODEL BEAMS

A. Theoretical model

This section reviews published work on generating the MGSM beams [21] in order to provide the context for the experiments presented in this paper.

The Schell-type cross-spectral density of a wide-sense statistically stationary random field at the planar source surface has form [17]

$$W^{(0)}(\rho_1, \rho_2; \omega) = \sqrt{S^{(0)}(\rho_1; \omega)} \sqrt{S^{(0)}(\rho_2; \omega)} \mu^{(0)}(\rho_2 - \rho_1; \omega) \quad (1)$$

where ρ_1 and ρ_2 are two-dimensional position vectors, ω is the angular frequency, $S^{(0)}$ is the spectral density and $\mu^{(0)}$ is the spectral degree of coherence in the source plane. For the MGSM beams $S^{(0)}$ and $\mu^{(0)}$ are chosen as

$$S^{(0)}(\rho; \omega) = e^{-\frac{\rho^2}{2\sigma(\omega)^2}} \quad (2)$$

where $\sigma(\omega)$ is the r.m.s. width of the source and

$$\mu^{(0)}(\rho_2 - \rho_1; \omega) = \frac{1}{C_0} \sum_{m=1}^M \binom{M}{m} \frac{(-1)^{m-1}}{m} e^{-\frac{|\rho_2 - \rho_1|^2}{2m\delta(\omega)^2}} \quad (3)$$

Here, C_0 is the normalization factor used for obtaining the same maximum intensity level for any number of terms, M is the upper summation index, $C_0 = \sum_{m=1}^M \binom{M}{m} \frac{(-1)^{m-1}}{m}$, $\binom{M}{m}$ is the binomial coefficient, and $\delta(\omega)$ is the r.m.s. correlation width.

At a distance z from the source plane the spectral density at any point (ρ, z) within the cross section of the MGSM beam has been shown to be [20]:

$$S(\rho, z; \omega) = W(\rho, \rho, z; \omega) = \frac{1}{C_0} \sum_{m=1}^M \binom{M}{m} \frac{(-1)^{m-1}}{m \Delta_m^2(z)} e^{-\frac{|\rho_2 - \rho_1|^2}{2\sigma^2 \Delta_m^2(z)}}, \quad (4)$$

where

$$\Delta_m^2(z) = 1 + \frac{z^2}{k^2 \sigma^2 \varrho_m^2} + \frac{2Tz^2}{k^2 \sigma^2}; \quad \varrho_m^2 = \left(\frac{1}{4\sigma^2} + \frac{1}{\delta_m^2} \right)^{-1}; \quad \delta_m = \sqrt{m} \delta; \quad T = \frac{1}{3} \pi^2 k^2 z \int_0^\infty \kappa^3 \Phi_n(\kappa) d\kappa \quad (5)$$

Here, $\Phi(\kappa)$ is the three-dimensional power spectrum of fluctuations in the refractive index of the isotropic random medium, κ is the spatial frequency and $k = \frac{2\pi}{\lambda}$ is the wave number.

The upper index M relates to the flatness of the intensity profile formed in the far field: $M = 1$ corresponds to the classical Gaussian Schell-Model source and $M \rightarrow \infty$ corresponds to sources producing far fields with flat centers and abrupt decays at the edges.

For any position or each pixel on the camera the scintillation index [SI] is defined as

$$SI = \frac{\langle X^2 \rangle}{\langle X \rangle^2} - 1, \quad (6)$$

where X is a time series of the fluctuating light intensity and $\langle \cdot \rangle$ represents the mean value.

B. Generating SLM screens

A reflective nematic Spatial Light Modulator (SLM) was used to create phase screen realizations compatible with the MGSM phase correlation (see section 2A). Papers [32, 35, 36] by Hyde et al., were referenced to create diffraction-shifted (MGSM) phase screens for use with a phase-only SLM with pixel resolution 256×256 . The phase correlation function is defined in [21] and given in eq. 3. Since Hyde's method is given in [32, 36], here we address only additional steps to reflect the experimental circumstances that pertain to our application. Figure 1 shows the measured intensities as a function of the beam radius for the experimental runs. For very small radii the values are noisy reflecting the fact that only a very few pixel values are used in the calculation of the radial intensity. As we expand the radius the averaging affect dominates the beam.

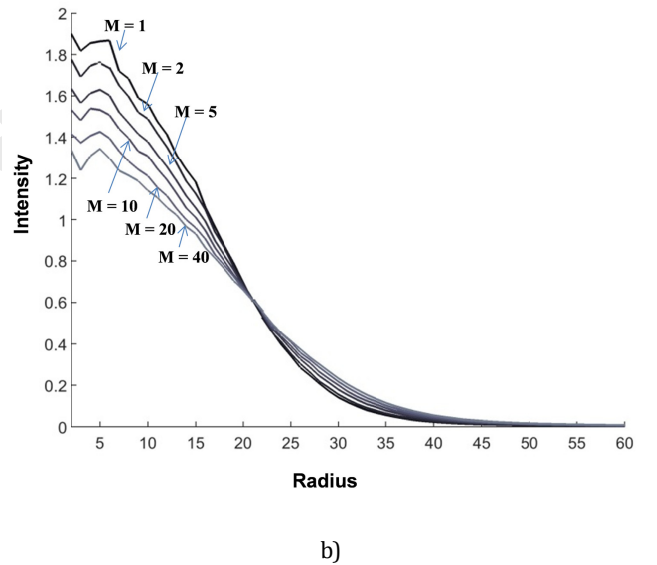
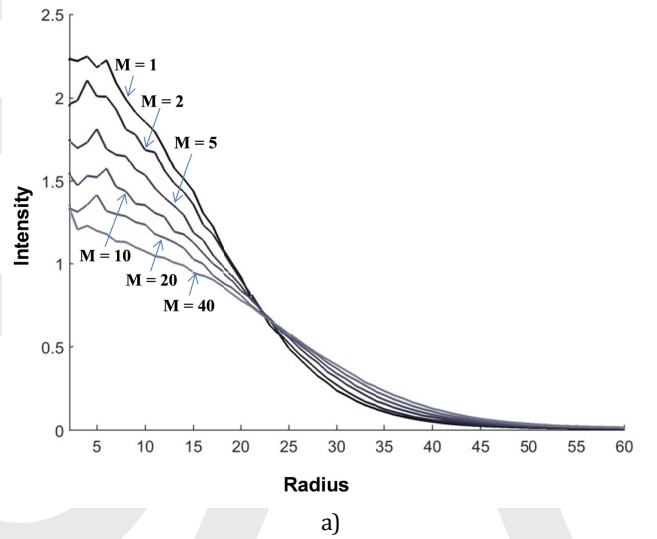


Figure 1. Radial intensity distribution for partially coherent beams with two different levels of coherence: a) $\delta^2 = 512 \text{ pixels}^2$ and b) $\delta^2 =$

1024 pixels², and with varying flatness factor $M = 1, 2, 5, 10, 20$ and 40 . Radius is given in mm.

Screen generation procedure sets the parameters from eq. 3 to vary M between 1 and 40, and δ^2 to be either 512 or 1024 pixels² (where each pixel width is 24 μm). We consider $M = 40$ to be representative of large M , and the choice of δ^2 is motivated by the necessity to deliver an adequate power level at the target considering the length of the propagation link.

Hyde's method for creating phase screens, ϕ_i , uses complex Gaussian variables and combines three phase contributions as follows (see the eq. 22 from [36]):

$$\phi_i = \text{mod}(G(h, d) + \phi_{i0} + F(h, d)) \quad (7)$$

where mod is remainder of division with 2π , ϕ_{i0} is the phase screen defined by eq. 3. $G(h, d)$ is a saw-tooth grating with height h , and $F(h, d)$ is a phase correction term that corrects the distortion that $G(h, d)$ induces in ϕ_{i0} , and d is the saw-tooth parameter which gives the period of the grid, in phase screen pixels, of the saw-tooth grating. We are only concerned with phase modulation and h does not vary with space so that correction $F(h, d)$ required by Hyde's method is constant in our application.

The saw-tooth grating causes power to be deposited primarily in the first diffraction order, which is displaced away from the zeroth order diffraction mode (the hotspot). The saw-tooth acts like a slight tilt of the SLM reflective surface. The MGSM diffractive phase screen pattern is then laid on top of the saw-tooth, causing the shifted beam to also change shape. The diffracted beam maintains the shape prescribed by the phase screen ϕ_{i0} , separating the hot spot and the beam.

We assume that the incident laser beam on the SLM has a Gaussian profile with radius ~ 1.5 mm. Hyde's method to modulate the effective amplitude by allowing h to vary spatially was not used. Hyde defines $E(h)$ is an algorithm parameter related to the ratio of the power sent to each diffracted mode. We fixed the ratio $E(h)/E(h = \text{lambda})$ at 0.7, seeking the maximum delivered power into the first diffraction mode and minimizing computational effort, and as such optimizing the power distribution in our experimental set up. We set d , the saw-tooth size parameter, to 8 pixels, and we set the saw-tooth axis on the 45 degree diagonal. A representative screen generated for our experiments using Hyde's method is given in Fig. 2.

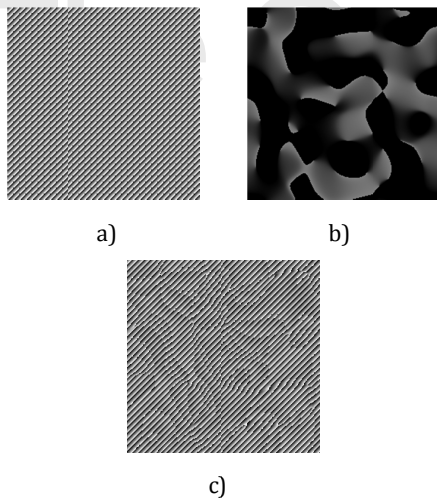


Figure 2. Representative screen generation: a) Saw tooth grating $G(h)$, b) phase mask ϕ_{i0} , c) SLM screen, ϕ_i . Screen parameters $\delta^2 = 512$ pixels², $M = 40$, SLM size 6.04 x 6.04 mm², Number of SLM pixels 256 x

256, saw-tooth parameter $d = 8$. $F(h, d)$ is not included in this figure since it is a constant phase shift in our scenario.

The Hyde's method convolves a specified window function, (eq. 3), with a field of white complex Gaussian noise. From the resulting smooth complex noise the amplitude is discarded and phase is kept.

C. Data analysis method

The data analysis in this paper follows the methods presented in [33], and only modifications that reflect experimental procedure used in the present effort are described in the following section.

In particular, the background intensity of the ambient was measured when the laser was completely blocked and subtracted from the measured intensity at every pixel at every frame. This step partially eliminates the bias in measurements due the manufacturer introduced variations in pixel's sensitivity to the light intensity. Camera data was taken by photographing a whiteboard with a lens rather than shooting the beam directly into the sensor. This step differs from the method presented in [33]. This led to three additional concerns: spatial inhomogeneity, lens vignetting, and lens distortion.

When shooting into the beam, the camera sensor area (4.736 mm x 3.552 mm) is small compared to the full "flattop" area of the developed beam (ten centimeters or larger). As a result, the time series of every pixel can be considered quasi-homogenous: while they have some speckle correlation, they see approximately the same intensity envelope. When recording with a lens, the field of view is much larger (30 cm), and this assumption is no longer valid.

To correct for this, and analyze only the on-axis and near-axis region of the beam, we created a mask of the beam area. The procedure for the mask creation is as follows: for each pixel, examine the background corrected mean intensity of the pixel time series, X and if X is greater than a prescribed threshold, ζ , pass that pixel on to analysis. Otherwise, if $X < \zeta$, omit the pixel. For each value of "flattop" parameter M , a different mask was generated. This procedure removes the off-axis dark region and passes only the circular region on-axis through for analysis. As the size and shape of the beam changes, from varying M or δ^2 , the exact size and shape of the mask also changes. This step was considered an acceptable compromise between measuring across the entire beam and not measuring the low intensity off-axis signal.

To address our second concern, lens vignetting, simplistically is caused when some light paths to the regions of the sensor are blocked by the lens system [34]. This can be seen as a reduction in signal intensity at pixels near the edge of the photograph of the beam and because of this extra precautions were implemented to center the beam on the photographs taken by the camera. While we were able to detect vignetting (especially in scintillation measurements), it is only significant far from the center of the beam. Because our masking technique only lets through pixels near the center of the beam, we ignored any signal distortion due to lens vignetting.

To address our third concern of lens distortion, the camera was oriented at a small angle with respect to the optical axis of the beam. The whiteboard was perpendicular to the optical axis. We ignored any distortion that may have been introduced by either geometric effects or non-ideal lens.

3. EXPERIMENTAL SET-UP

The experimental set-up used a simple layout with a laser beam from a red HeNe laser source, expanded and collimated to cover the reflective surface of the SLM (see Fig. 3). All of the reflected light from the SLM screen is modulated due to the 100% fill factor [37]. The generated MGSM beam was propagated for 70 m in weak turbulence in air. The beam on the target was photographed on a white board using a

camera with a suitable lens. The experimental procedure consisted of photographing the beam intensity using camera at the rate of 10 frames per second. Beams were generated from a pool of 8000 phase screens with the same statistics and cycled on an SLM with the rate of 333 screens per second. This step assured close to theoretical statistics with the fastest possible rate of change utilized to create spatially pseudo-partially coherent beams. An initial background measurement was taken, and subsequently for each M value a 30 second movie was recorded. We selected $M = 1$ to create a reference Gaussian Schell model beam and then increased M to 2, 5, 10, 20 and 40 to embody the increasing beam flatness for the MGSM. We tested the beams with $\delta^2 = 512$ pixels² and $\delta^2 = 1024$ pixels² to provide the variety of the coherence level and to realistically capture the beam intensity necessary for scintillation analysis.

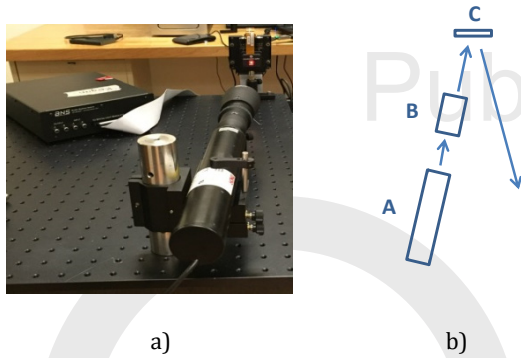


Figure 3. Experimental set up. A - laser source, B - beam expander, C - SLM. a) Instrumentation and b) schematic set up.

4. RESULTS

Measurement results are summarized by first establishing the scope of the performed experiments to include beams with suitable directionality that clearly exhibit the scintillation index dependence on beam shape over the experimental link. Next, the scintillation measurements as a function of M , demonstrate the successful investigation in scintillation index reduction for larger values of M .

Fig. 4 presents the measured intensity of the laser beam after propagating 70 m and the mask used to differentiate the laser light from background on the beam photograph. Additionally, we show the scintillation index vs. pixel-intensity point clouds as justification that there are no systematic errors due to camera gain. There is no significant correlation between the measured laser light intensities and the calculated scintillation.

We introduce a mask to isolate only the part of the beam that is bright enough for reliable calculations. The final results are averaged over the area of the mask (Fig. 5).

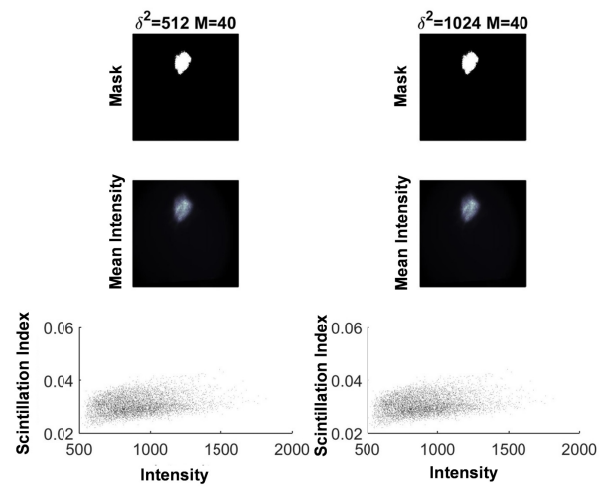


Figure 4. Applied mask with a threshold, ζ , of 350 to extract only intensity region on the photograph, suitable for scintillation index analysis (top row). Mean beam spatial intensity distribution photographed at target (middle row). Point cloud plots to demonstrate independence of scintillation index calculations from the beam intensity (bottom row). Left column $\delta^2 = 512$ pixels² and right column $\delta^2 = 1024$ pixels², $M = 40$.

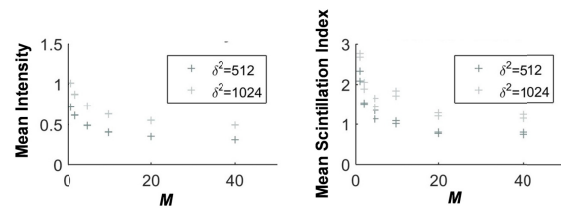


Figure 5. a) Measured mean normalized intensity and b) Calculated mean scintillation index within the mask as a function of changing M .

5. CONCLUSIONS

In this work, we present to our knowledge, the first experimental verification of the fact that not only the typical width of the source correlation function but also its shape can reduce the scintillation index of a beam propagating in atmospheric turbulence. The family of the MGSM beams that we have used presented a great opportunity for this: since each beam of this type being depends on two parameters, the r.m.s. correlation width and the flatness parameter. We have investigated the scintillation index of the beams with the same values of the r.m.s. widths but different values of flatness parameter and found that for larger values of the latter the scintillation index reduces substantially, in agreement with previous analytical results and computer simulations.

While for one-parametric model sources (like the GSM sources) the minimization of the scintillation index can be done solely by tuning the correlation width, as is seen from our results, for two-parametric models (like MGSM sources) the two-step optimization is needed, in terms of the correlation width and then in terms of the flatness parameter.

Our results might find applications in free space optical communication systems which involve short-link atmospheric channels and low power laser sources.

Funding sources and acknowledgments. S. Avramov-Zamurovic and S. Guth are supported by US ONR grant: N0001414-WX-00267. C.

Nelson is supported by US ONR grant N0001414WX20723. O. Korotkova is supported by the Air Force Office of Scientific Research (AFOSR) grant FA9550-12-1-0449; and the Office of Naval Research (ONR) grant N00014-15-1-2350.

References

1. J. H. Churnside, "Aperture averaging of optical scintillations in the turbulent atmosphere," *Appl. Opt.* 30, 1982-1994 (1991).
2. X. Zhu and J. M. Kahn, "Free-space optical communication through atmospheric turbulence channels," *IEEE Trans. On Communications* 50, 1293-1300 (2002).
3. A. Peleg and J. Moloney, "Scintillation reduction by use of multiple Gaussian laser beams with different wavelengths," *Photonics Technology Letters* 19, 883-885 (2007).
4. Y. Gu, O. Korotkova and G. Gbur, "Scintillation of non-uniformly polarized beams in atmospheric turbulence", *Opt. Lett.* 34, 2261-2263 (2009).
5. J. C. Leader, "Intensity fluctuations resulting from partially coherent light propagating through atmospheric turbulence," *J. Opt. Soc. Am.* 69, 73-84 (1979).
6. V. A. Banakh, V. M. Buldakov, and V. L. Mironov, "Intensity fluctuations of a partially coherent light beam in a turbulent atmosphere," *Opt. Spektrosk.* 54, 1054-1059 (1983)
7. R. L. Fante, "Intensity fluctuations of an optical wave in a turbulent medium; effect of source coherence," *Opt. Acta* 28, 1203-1207 (1981).
8. J. Wu, "Propagation of a Gaussian-Schell beam through turbulent media," *J. Mod. Opt.* 37, 671-684 (1990).
9. O. Korotkova, L. C. Andrews, R. L. Phillips, "A Model for a Partially Coherent Gaussian Beam in Atmospheric Turbulence with Application in LaserCom", *Opt. Eng.* 43, 330-341 (2004).
10. J. C. Ricklin and F. M. Davidson, "Atmospheric optical communication with a Gaussian-Schell beam," *J. Opt. Soc. Am. A* 20, 856-866 (2003).
11. T. J. Schulz, "Optimal beams for propagation through random media," *Opt. Lett.* 30, 1093-1095 (2005).
12. R. L. Fante, "The effect of source temporal coherence on light scintillations in weak turbulence," *J. Opt. Soc. Am.* 69, 71-73 (1979).
13. G. P. Berman, A. R. Bishop, B. M. Chernobrod, V. N. Gorshkov, D. C. Lizon, D. I. Moody, D. C. Nguyen and S. V. Torous, "Reduction of laser intensity scintillations in turbulent atmospheres using time averaging of a partially coherent beam," *J. Phys. B*, 42, 225403 (2009).
14. F. Gori, G. Guattari, and C. Padovani, "Modal expansion for J0-correlated Schell-model sources," *Opt. Commun.* 64, 311-316 (1987).
15. S. A. Ponomarenko, 2001. "A class of partially coherent beams carrying optical vortices," *J. Opt. Soc. Am. A*, 18, 150-156 (2001).
16. H. Lajunen and T. Saastamoinen, "Propagation characteristics of partially coherent beams with spatially varying correlations," *Opt. Lett.* 36, 4104-4106 (2011).
17. S. Sahin, O. Korotkova, "Light sources generating far fields with tunable flat profiles", *Opt. Lett.* 37, 2970-2972 (2012).
18. Z. Mei and O. Korotkova, "Random sources generating ring-shaped beams", *Opt. Lett.* 38, 91-93 (2013).
19. Z. Mei and O. Korotkova, "Cosine-Gaussian Schell-model sources", *Opt. Lett.* 38, 2578-2580 (2013).
20. O. Korotkova, "Random sources for beams with rectangular symmetry", *Opt. Lett.* 39, 64-67 (2014).
21. O. Korotkova, S. Sahin, E. Shchepakina, "Multi-Gaussian Schell-model beams", *J. Opt. Soc. Am. A* 29, 2159- 2164 (2012).
22. Z. Tong and O. Korotkova, "Non-uniformly correlated beams in uniformly correlated random media", *Opt. Lett.*, 37, 3240-3242 (2012).
23. Z. Mei, E. Shchepakina and O. Korotkova, "Propagation of Cosine-Gaussian Schell-model beams in atmospheric turbulence", *Opt. Express* 21, 17512-17519 (2013).
24. J. Cang, P. Xiu, X. Liu, "Propagation of Laguerre-Gaussian and Bessel-Gaussian Schell-model beams through paraxial optical systems in turbulent atmosphere" *Optics & Laser Technology* 54, 35-41, (2013).
25. O. Korotkova and E. Shchepakina, "Rectangular Multi-Gaussian Schell-model beams in free space and the atmosphere," *J. Opt.* 16, 145704 (2014).
26. Y. Yuan, X. Liu, F. Wang, Y. Chen, Y. Cai, J. Qu, and H. T. Eyyuboğlu. "Scintillation index of a multi-Gaussian Schell-model beam in turbulent atmosphere," *Opt. Commun.* 305, 57-65 (2013).
27. O. Korotkova, S. Avramov-Zamurovic, C. Nelson, R. Malek-Madani, Y. Gu, and G. Gbur, "Scintillation reduction in multi-Gaussian Schell-model beams propagating in atmospheric turbulence", *Proc. SPIE 9224, Laser Communication and Propagation through the Atmosphere and Oceans III, 92240M* (October 3, 2014).
28. F. Wang, C. Liang, Y. Yuan, and Y. Cai, "Generalized multi-Gaussian correlated Schell-model beam: from theory to experiment," *Opt. Express* 22, 23456-23464 (2014).
29. Y. Chen, F. Wang, L. Liu, C. Zhao, Y. Cai and O. Korotkova, "Generation and propagation of a partially coherent vector beam with special correlation functions," *Phys. Rev. A*, 89, 013801 (2014).
30. C. Liang, X. Liu, F. Wang, Y. Cai and O. Korotkova, "Cosine-Gaussian-correlated Schell-model beams with rectangular symmetry", *Opt. Lett.* 39, 769-772 (2014).
31. S. Avramov-Zamurovic, O. Korotkova, C. Nelson, O. Korotkova and R. Malek-Madani, "The dependence of the intensity PDF of a random beam propagating in the maritime atmosphere on source coherence," *Waves in Complex and Random media* 24, 69-82 (2014).
32. M. W. Hyde IV, S. Basu, X. Xiao, and D. Voelz, "Producing any desired far-field mean irradiance pattern using a partially-coherent Schell-model source," *J. Opt.* 17 055607 (2015)
33. S. Avramov-Zamurovic, C. Nelson, S. Guth, O. Korotkova, R. Malek-Madani, "Experimental study of electromagnetic Bessel-Gaussian Schell Model beams propagating in a turbulent channel", *Optics Communications*, Volume 359, 15 January 2016, Pages 207-215
34. S. Chen, S. Dai, and P. Mu, Correction of CCD camera lens vignetting, *Applied Mechanics and Materials Vols. 373-375* (2013) pp 603-607, 2013/Aug/30, doi:10.4028/www.scientific.net/AMM.373-375.603
35. M. W. Hyde, S. Basu, X. Xiao, and D. G. Voelz "Producing any desired far-field mean irradiance pattern using a partially-coherent Schell-model source and phase-only control", *Imaging and Applied Optics 2015 OSA Technical Digest* (online) (Optical Society of America, 2015), paper PW3E.2.
36. M. W. Hyde, S. Basu, D. G. Voelz, and X. Xiao, "Experimentally generating any desired partially coherent Schell-model source using phase-only control", *J. Appl. Phys.* 118, 093102 (2015);
37. Spatial Light Modulators – XY Series, manufacturer specifications: <http://bnonlinear.com/pdf/XYSeriesDS0909.pdf>